Theory of elastic constants of cubic transition metals and alloys

Per Söderlind
Department of Physics, Uppsala University, Uppsala, Sweden

Olle Eriksson,* J. M. Wills, and A. M. Boring
Center for Materials Science and Theoretical Division, Los Alamos National Laboratory, Los Alamos, New Mexico 87545
(Received 7 December 1992; revised manuscript received 15 March 1993)

We have from first principles calculated the elastic constants (C_{11}, C_{12}, and C_{44}) of all nonmagnetic cubic d transition metals, and obtained good agreement with experimental data. We show that the trend exhibited by the tetragonal shear constant in the transition metals can be simply understood. In particular, we show that *the trend of the tetragonal shear constant, C', of cubic transition metals and alloys is determined by the energy difference between the fcc and bcc structures of a given system, which in turn is determined by band filling.* This finding is in turn due to the result that these systems have a Bains path with similar shape, and our "canonical" Bains path illustrates this behavior. The trend of C' is further studied by including selected alloys (thereby obtaining a finer tuning of band-filling effects). The scaling of C' with the bcc-fcc energy difference is found to hold also for the studied alloys (roughly), and the calculated C' is found to agree well with available experimental data.

I. INTRODUCTION

Most ground-state properties of the transition metals are now well characterized and understood. For instance, the equilibrium volume (V_{eq}) shows a parabolic trend with a minimum approximately in the middle of the series. Also, the bulk modulus (B) and the cohesive energy (E_c) have similar trends, but with a maximum approximately where the volume has a minimum. These trends are roughly given by the Friedel model;[1,2] in which one is occupying bonding d orbitals in the first half of the series and then filling antibonding d orbitals in the second half of the series. In this model the d orbitals form a narrow band that is pinned at the Fermi energy (E_F). A more quantitative picture of the trends of all three quantities is given by the universal bonding model[3,4] based upon local-density approximation (LDA) calculations. An important feature of the LDA calculations is that B, V_{eq}, and E_c can be determined within 10% independent of crystal structure, indicating these quantities are independent of the arrangement of the atoms as long as they are rather closely packed (fcc, bcc, or hcp). It is this blend of detailed calculations (LDA results) and descriptive concepts (Friedel model) that has given a deeper understanding of these average properties of solids.

In contrast to the clear parabolic trends of the cubic transition metals, shown by V_{eq}, B, and E_c, is the behavior of the elastic constants (C', C_{11}, C_{12}, and C_{44}). Since the observed elastic constant trends for the 3d, 4d, and 5d series are similar, we will focus the discussion mainly on the 5d series. To illustrate the problem we show in Fig. 1 the experimental tetragonal shear constants C' and the bulk moduli B [$C'=(C_{11}-C_{12})/2$ and $B=(C_{11}+2C_{12})/3$] for the 5d series. We also show the calculated trend of C' using ion-ion potentials.[5] We have chosen C' instead of C_{11} or C_{12} because this constant is obtained from the curvature of the total energy for a tetragonal distortion of a cubic lattice (see below). Despite the fact that C' and B are both linear combinations of C_{11} and C_{12}, they do not follow a similar trend; the shear constants of W and Ir are highly anomalous,

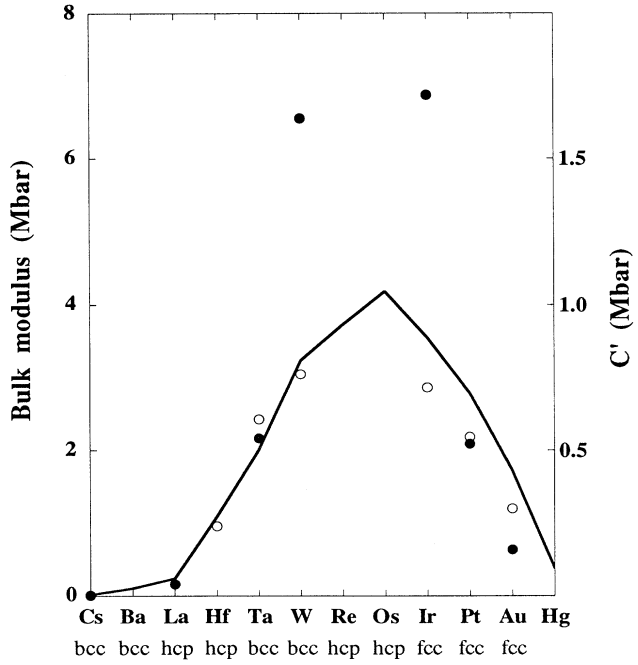

FIG. 1. Experimental data for the tetragonal shear constant (solid circles, right-hand scale) and for the bulk modulus (solid line, left hand scale), of the 5d transition metals. Also shown are calculated values of C' using ion-ion potentials (open circles, right-hand scale).

while the shear constants of Cs, La, Ta, Pt, and Au follow approximately the same trend as B. Notice also that calculations of C' using ion-ion potentials reproduce the trend of B, instead of C' and thus fail to reproduce the experimental data for W and Ir. The lack of a simple parabolic behavior for the trend of C' has led to the belief that there is no simple explanation of elastic constant behavior in the transition-metal elements. Similar, although not as pronounced, effects can also be found for C_{44}.

Many previous studies of elastic properties of transition-metal elements have mainly demonstrated the complexity of the behavior. For example, the high shear constant of Ir yields unusual brittle cleavage of that material, and it was argued on this basis that Ir has very strong directional atomic binding forces.[6] Similarly, using interatomic central force potentials, it has been argued that the bcc transition elements have strong directional covalent bonds, since C' and E_c could not both be fitted.[7] The directionality in the bonds of bcc metals was also used as an argument for the similar behavior of ΔE_0 and K_b^7 (ΔE_0 is the deviation between the predicted cohesive energies with and without the presence of covalent bonds, and K_b is proportional to the difference between calculated and experimental C' values). Moreover, the covalent bond strength was suggested to decrease with increasing $|n_d-5|$, where n_d is the number of d electrons.[7]

In an earlier paper we demonstrated a simple correlation between C' and the magnitude of the fcc-bcc crystal structure energy difference,[8] which from hereafter is referred to as ΔE. The tetragonal shear constant C' is obtained from the curvature of the total energy under a volume conserving deformation that modifies the z axis but keeps the x and y axes equal, while conserving volume.[9–11] C' is obtained from the curvature around the energy minimum, i.e., for very small shears. However, the same shear (tetragonal), although larger, can transform a bcc crystal to a fcc crystal and vice versa. Hence, both the fcc and bcc crystal can be described as body-centered tetragonal with c/a equal to $\sqrt{2}$ and 1, respectively. This kind of shear is referred to as the Bains transformation path.[12] It is therefore illustrative to study the total energy as a function of not only small shears (the C' values), but also shears of larger magnitude that bring a bcc crystal to the fcc structure and vice versa. These considerations indicate that an understanding of C' is tied up with an understanding of crystal structure trends in the transition metals. The present study extends the earlier work to include all cubic, nonmagnetic transition metals and their alloys and includes a discussion of the trends or lack thereof of C_{44}.

The crystal structure stabilities of most of the transition metals have been calculated from first principles.[13–15] The trend of the crystal structure stabilities was shown to be determined by the d electrons, and it was even demonstrated that the eigenvalues [and therefore the density of states (DOS)] of the "canonical d bands"[16,17] (which only depend on the crystal structure, with no potential nor volume dependence) describe these trends.[13,14] The dominant term in minimizing the total energy of a given structure is associated with the shape, and the filling (number of valence electrons) of the partial d DOS. This is essentially described by the canonical d bands, which are unique to that particular arrangement of the atoms. To illustrate this we show in Fig. 2 the canonical d DOS for the fcc and bcc structures. In Fig. 3 we show the difference between the first moment (eigenvalue sum) of the two DOS. The band energy E_b (first moment) of the d electrons is defined as

$$E_b=\int_{-\infty}^{E_F}\epsilon N(\epsilon)d\epsilon\ , \tag{1}$$

where N is the canonical d DOS. Notice in Fig. 3 that the fcc energy is the reference level, and is set to zero. Figure 3 suggests that initially the fcc structure is stable, then for d-band fillings between ~ 3 and ~ 5 the bcc structure is stabilized, and for between ~ 5 and ~ 9 d electrons the fcc structure is stabilized again. A similar analysis was presented earlier[13,14] including also the hcp structure. The crystal structure trends exhibited by the transition metals can thus be explained using the above stated simple arguments; in the 5d series La and Hf (d-band filling ~ 1.5–2.5) are close packed (hexagonal), Ta and W (d-band filling ~ 3.5–4.5) are bcc, whereas the rest of the series is close packed (hcp or fcc). The reason for the trend of the first moment (Fig. 3) can be seen in Fig. 2. Namely, it is energetically favorable to have as much weight of the DOS pushed to lower energies compared to E_F. For d-band fillings around 4 to 5, E_F lies between -3 and 0 in Fig. 2, and the bcc structure is thus stabilized.

We turn to the detailed LDA calculations of the elastic constants themselves which indicate the level of accuracy that can be obtained. An *ab initio* calculation of elastic constants of transition metals was presented by Dacorogna, Ashkenazi, and Peter,[9] who calculated the C' constants for 13 fcc and bcc transition metals, using the linear muffin-tin orbital method in the atomic sphere approximation (LMTO-ASA).[16,17] These results compared fairly well with experiments, with the largest disagreement being $\sim 50\%$ to large in fcc Pd, $\sim 60\%$ to large in

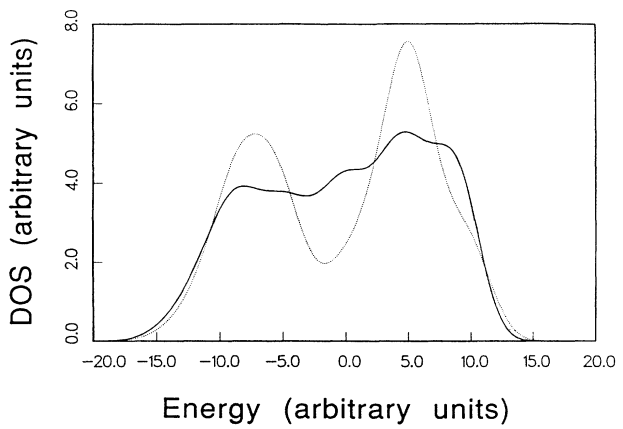

FIG. 2. Canonical d DOS for the fcc (full drawn line) and bcc (dotted line) structure. The DOS was convoluted with a Gaussian function.

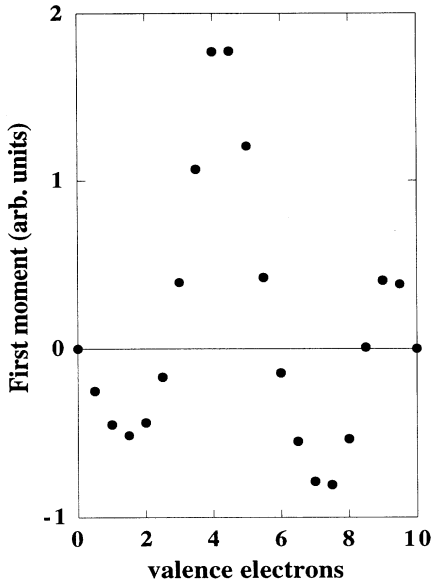

FIG. 3. Calculated difference between the first moment of the fcc and bcc structures. The bcc moment is the reference level and is set to zero.

fcc Ag, as well as ~60% to large in bcc Mo. Christensen[10] on the other hand found good agreement for both fcc Pd and fcc Au, using LMTO-ASA calculations. Moreover, Shimizu[18] and Ohta and Shimizu[19] found fairly poor agreement in their calculated C' constants of V and Cr. The only full-potential treatment of elastic constants of transition elements, that we are aware of, were published by Alouani, Albers, and Methfessel who obtained good agreement with experiment for bcc Mo.[20]

II. DETAILS OF CALCULATIONS

As mentioned above there are only three elastic constants in a cubic material (neglecting the bulk modulus); C_{11}, C_{12}, and C_{44}. These constants can be obtained by calculating the total energy as a function of the shears described below.[9–11] For C_{11} and C_{12} one considers the following shear:[9–11]

$$\begin{bmatrix} 1+\delta & 0 & 0 \\ 0 & 1+\delta & 0 \\ 0 & 0 & \dfrac{1}{(1+\delta)^2} \end{bmatrix}, \tag{2}$$

i.e., modifying the z axis, but keeping the x and y axes the same, in a volume conserving way. The change in strain energy density as a function of the shear δ is then

$$U = 6C'\delta^2 + O(\delta^3), \tag{3}$$

where C' is the tetragonal shear constant, $C' = \frac{1}{2}(C_{11} - C_{12})$. By calculating C' and the bulk modulus $B = \frac{1}{3}(C_{11} + 2C_{12})$, one can extract C_{11} and C_{12}. Similarly, considering the following shear:[9–11]

$$\begin{bmatrix} 1 & \delta & 0 \\ \delta & 1 & 0 \\ 0 & 0 & \dfrac{1}{1-\delta^2} \end{bmatrix}, \tag{4}$$

the C_{44} constant can be calculated from

$$U = 2C_{44}\delta^2 + O(\delta^4). \tag{5}$$

The strain energy density is the increase of the energy density of a distorted system, which is proportional to the corresponding change in total energy. In order to calculate the total energy for a given shear, we have used a full-potential linear muffin-tin orbital method[21] (FP-LMTO) as well as an LMTO-ASA (Refs. 16 and 17) method. The accuracy of the total-energy differences needed for calculating the elastic constants is $\sim\mu$Ry, and as we shall see one needs a highly accurate computational method (FP-LMTO) to obtain good agreement with experimental data. However, it is interesting that the trends of the elastic constants can be well reproduced[10] using the less accurate LMTO-ASA method and we will discuss this finding below.

Most of the details of the FP-LMTO calculations were similar to previous calculations. However there are some aspects of these types of calculations that are not "standard." One of the most problematic issues is the convergence of the **k**-space sampling. We have used the special **k**-point method[22] in this work, to speed up **k**-space convergence. In addition to this we have associated each eigenvalue used in the calculations with a Gaussian having a width ~15 mRy. We have tested this approach for selected systems and found that it accelerates the convergence, with negligible changes in the calculated elastic properties. For the present calculations we then sampled the $\frac{1}{16}$ [Eq. (2)] and the $\frac{1}{8}$ [Eq. (4)] irreducible part of the Brillouin zone, with **k** points that both correspond to 4000 points in the full zone for the fcc lattice, and 4000–5324 points for the bcc lattice.

The LMTO-ASA calculations were the same as in Skrivers previous work,[13] although we used s, p, d, and f partial waves. These calculations were only done to give additional and complementary information of the C' values. Both types of calculations (full-potential and ASA) were based on the local-density approximation, with only crystal structure and nuclear charge as input.

III. RESULTS

A. Metals

Shown in Tables I and II are the calculated (FP-LMTO, using the experimental crystal structure) and experimental values of C_{11}, C_{12}, and C_{44} for all nonmagnetic cubic transition metals. Notice that with a few exceptions we have agreement between experiment and theory within ~10% for all three elastic constants. It should be noticed here that La is stabilized in the fcc structure only at elevated temperatures. The worst agreement between theory and experiment is found for the C_{44} constant of bcc V. We note that for V, LDA gives less accurate re-

TABLE I. Experimental and theoretical values of C_{11} and C_{12} (in Mbar). The experimental value of fcc La was obtained at elevated temperatures ($\sim 600\,^{\circ}C$).

		C_{11}^{theor}	C_{12}^{theor}	C_{11}^{expt}	C_{12}^{expt}
5*d*	La (fcc)	0.29	0.17	0.29	0.20
	Ta (bcc)	2.91	1.62	2.66	1.58
	W (bcc)	5.53	2.07	5.33	2.05
	Ir (fcc)	6.20	2.65	6.00	2.56
	Pt (fcc)	3.72	2.53	3.58	2.54
	Au (fcc)	2.09	1.75	2.02	1.70
4*d*	Nb (bcc)	2.67	1.47	2.53	1.33
	Mo (bcc)	4.06	1.50	4.50	1.73
	Rh (fcc)	3.97	1.71	4.13	1.94
	Pd (fcc)	1.95	1.67	2.34	1.76
	Ag (fcc)	1.28	0.86	1.32	0.97
3*d*	V (bcc)	2.05	1.30	2.32	1.19
	Cu (fcc)	1.93	1.51	1.76	1.25

sults also for other properties, e.g., the equilibrium volume is $\sim 10\%$ to small[23] (the equilibrium volume can normally be obtained within $\sim 6\%$). We therefore performed a calculation of C_{44} at the theoretical volume of V, and the agreement with experiment is improved, 0.30 Mbar, whereas for the C_{11} and C_{12} constants the agreement is worse, 3.10 and 1.63 Mbar, respectively. Notice also that the isoelectronic fcc metals Rh, and Ir have anomalously high C_{11} values. A similar situation is found for bcc Mo and W. These high constants come about, since the curvature of the total energy for a tetragonal strain (C') is particularly large for these systems.[8] The bulk modulus, which together with C' is used to calculate C_{11} and C_{12}, behaves more smoothly (Fig. 1). In our previous report[8] on elastic constants of 5*d* transition metals we found agreement within $\sim 10\%$ for the C' values, and we demonstrated that the anomalies found in Ir (Rh) and W (Mo) is a reflection of the anomalously high ΔE found in these systems. The anomalously high values of C_{11}, for Ir, Rh, W, and Mo is thus a reflection of the unusually large tetragonal shear constant found for these systems.[8] Table II suggests that also C_{44} has slightly larger values for Ir, Rh, W, and Mo, compared to the trend expected for the bulk modulus (as well as volume and cohesive energy). However the strain that corresponds to the C_{44} constant is more complicated and we have not found correlations with other properties, as is the case for C'. We will return to discussions of C_{44} in Sec. III B.

TABLE II. Experimental and theoretical values of C_{44} (in Mbar). The experimental value of fcc La was obtained at elevated temperatures ($\sim 600\,^{\circ}C$).

		C_{44}^{theor}	C_{44}^{expt}
5*d*	La (fcc)	0.16	0.17
	Ta (bcc)	0.84	0.87
	W (bcc)	1.78	1.63
	Ir (fcc)	2.66	2.68
	Pt (fcc)	0.85	0.77
	Au (fcc)	0.31	0.45
4*d*	Nb (bcc)	0.27	0.31
	Mo (bcc)	1.07	1.25
	Rb (fcc)	1.96	1.84
	Pd (fcc)	0.73	0.72
	Ag (fcc)	0.61	0.51
3*d*	V (bcc)	0.05	0.46
	Cu (fcc)	0.82	0.82

The unusual behavior for C_{11} (and C_{12}) is thus a reflection of the behavior of the tetragonal shear constant, and we have done some additional analysis of this property. As stated above it is illustrative to study not only small strains in Eq. (1), but the entire Bains path.[8] The total energies are shown in Fig. 2 of Ref. 8 (obtained from LMTO-ASA) for all 5*d* elements (including the hexagonal ones, treated as fcc to illustrate trends) as a function of c/a ratio, i.e., the calculated Bains path [with the reference energy set to zero for $c/a = \sqrt{2}$, (fcc) for all elements]. From that figure it is clear that systems that have a large ΔE show a large curvature of the total energy around the energy minimum (both for bcc and fcc crystals) and should therefore show large C' values. That figure thus suggests that *C' scales with the energy difference between the bcc and fcc structures.* To test this hypothesis, we show in Fig. 4 the calculated [LMTO-ASA (a) and FP-LMTO (b)] C' values, as well as ΔE, for all 5*d* metals (including the hexagonal ones, treated as fcc to illustrate trends). We have also plotted the experimental data for the cubic metals in Fig. 4. Notice that *the anomalously high shear constants of W and Ir simply reflect a very large difference in crystal structural energies.* Similarly this explains the high C' values of Mo and Rh in the 4*d* series. The reason for these large differences in crystal structure energies have previously been demonstrated to be governed by the *d*-band filling, and in particular the shape of the canonical *d* bands (Figs. 2 and 3).[13,14] Notice also that the scaling between the crystal

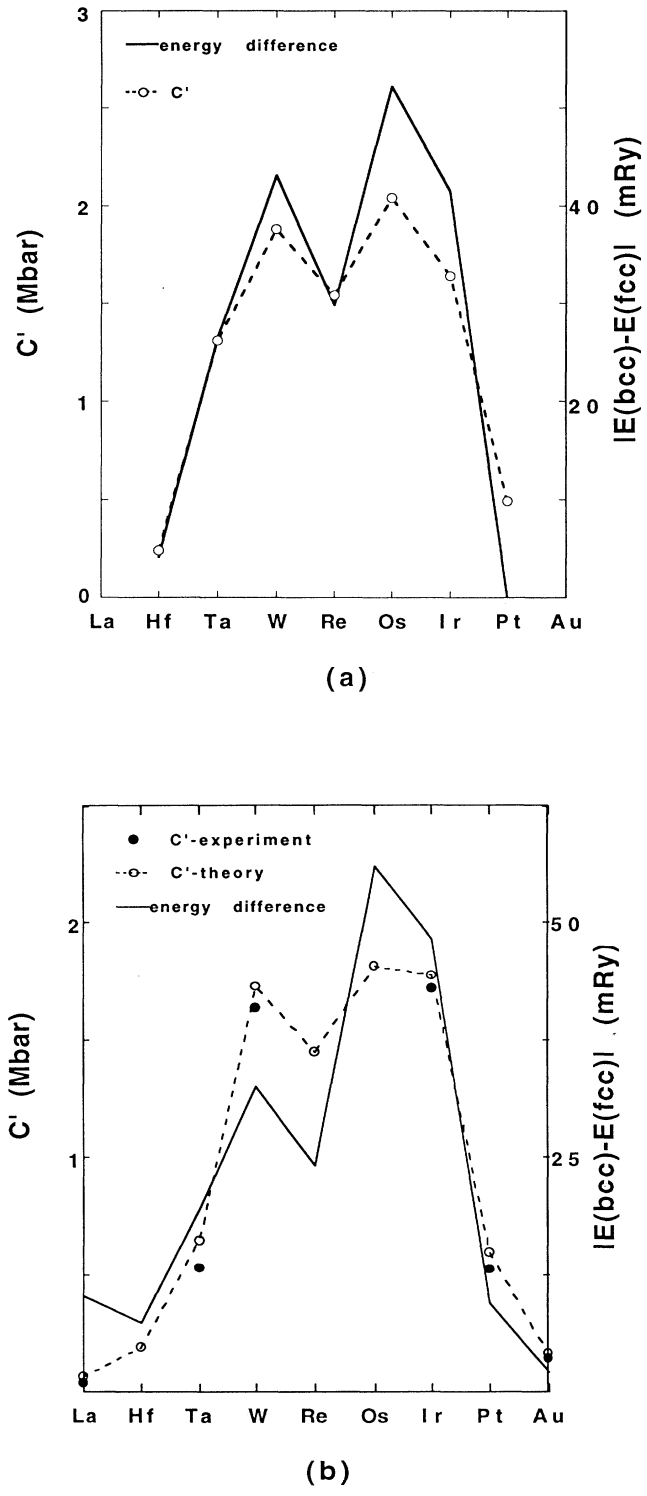

FIG. 4. Theoretical data for the absolute value of the energy difference between the fcc and bcc structures (full drawn line, right-hand scale), as well as the calculated tetragonal shear constant, C' (open circles, left-hand scale). The LMTO-ASA results are shown in (a) and the FP-LMTO results in (b). The experimental data for C' are also shown (b) (filled circles).

structure energy and C' depends on the shape of the Bains path for a particular system. However, it is seen that (except for the high-temperature phase of La) there is agreement within 10–20 %.

The scaling between C' and ΔE is interesting, and we have done some additional analysis concerning this issue. Therefore we show in Fig. 5 the canonical DOS for the bct structure as function of c/a ratio. Notice that as the c/a ratio is changed continuously the resulting DOS, and therefore also the first moment E_b [Eq. (1)], varies smoothly. Starting at $c/a=0.8$ the DOS looks like a distorted version of the bcc DOS. Increasing c/a towards 1.0, makes the similarity more pronounced. For c/a ratios increasing from 1 the gap between the two bcc peaks (E_g and T_{2g}) starts to get filled and the DOS becomes

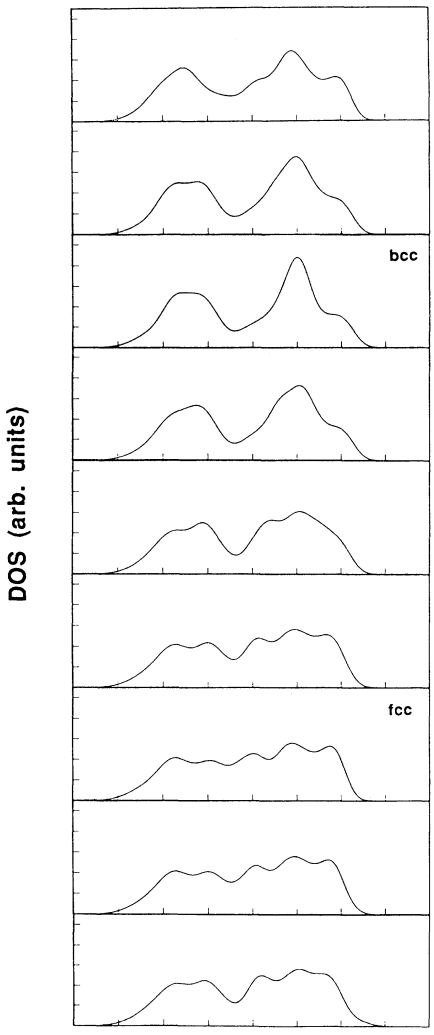

FIG. 5. Canonical d DOS for the bct structure using a c/a ratio of 0.8 (upper panel) to 1.6 (lower panel). The special cases $c/a=1$, and $c/a=\sqrt{2}$ correspond to the bcc and fcc structures, respectively. The DOS was convoluted with a Gaussian function.

more fcc like. Increasing c/a from $\sqrt{2}$ (fcc) produces a gap in the middle of the DOS again. To further elaborate on this, we show the canonical Bains path in Fig. 6, for d-band fillings with 3 ($\sim$Ta), 4 ($\sim$W), and 7 ($\sim$Ir) electrons. These paths were calculated from the first moment [Eq. (1)] of the d DOS curves in Fig. 5. However the different paths were scaled to have the same energy difference between the fcc and bcc structures (ΔE), and were also shifted to lie at the same energies. Thus the energy scale in Fig. 6 has no meaning, but the shape of the curves has. It is striking from Fig. 6 that the shape of the Bains path is very similar irrespective of crystal structure and band filling. However, one should bear in mind that for these band fillings ΔE is very large and that this partly explains the similar shape of the canonical Bains paths. For other band fillings, where ΔE is smaller, the canonical Bains path differs slightly from the universal behavior suggested by Fig. 6. Also, other contributions to the total energy show a different behavior, and specifically the Madelung contribution wants to stabilize high symmetry structures, $c/a=1$ and $\sqrt{2}$. Therefore, depending on which terms dominate the energy along the Bains path can deviate from a "universal" behavior, and this is in fact the explanation to why the scaling between C' and ΔE is not perfect (Fig. 4). Nevertheless, systems where E_b dominates show a total energy along the Bains path that is quite similar in shape.

In order to illustrate the Madelung contribution to the total energy we show in Fig. 7 an estimate of this contribution, for La, Re, and Au. This energy was calculated according to the formula of Esposito *et al.*,[24,13] i.e.,

$$U_M=-\frac{1}{2}(q_s|e|)^2\frac{\alpha_M-1.8}{S}\ , \tag{6}$$

where α_M is the Madelung constant of the lattice and S is the atomic Wigner-Seitz radius. Further, $q_s|e|$ is obtained from our LMTO-ASA energies through

$$q_s|e|=\tfrac{4}{3}\pi S^3 n(S)|e|\ , \tag{7}$$

where $n(S)$ is the electron density at the atomic radius. Notice in Fig. 7 that the Madelung energy stabilizes high symmetry structures, i.e., the bcc and fcc structures along the Bains path. Notice also that the Madelung energy has a larger energy barrier between the bcc and fcc structures, for systems in the middle of a series (Re in our example). We will return to this results in Sec. III B.

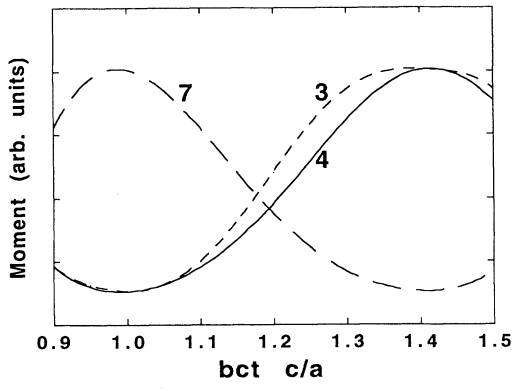

FIG. 6. Canonical Bains path for d-band fillings of 3 (short-dashed line), 4 (full drawn line), and 7 (long-dashed line).

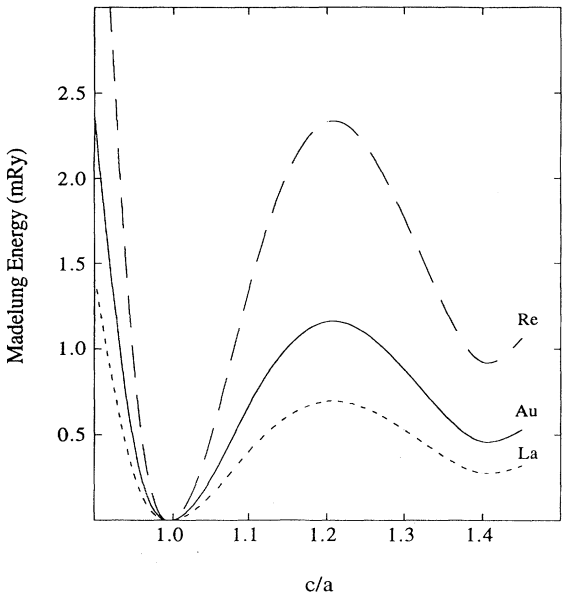

FIG. 7. Madelung energy [Eqs. (6) and (7)] for the Bains path of La, Re, and Au.

B. Alloys

In the preceding section it was argued that the elastic shear constant, C', scales with the fcc-bcc energy difference, ΔE, and that this holds for systems that display a similar shape of the Bains path. Using these arguments it then follows that systems where band filling dictates a low (or zero) ΔE should display a low C' constant. Hence, since the crystal structure stability between the bcc and fcc structure changes sign somewhere between Mo and Tc in the 4d series, and somewhere between W and Re in the 5d series, it is interesting to study the behavior of C' for MoTc alloys and WRe alloys. In order to study a successive filling of the d band we have calculated the structural energy difference for these alloys using the virtual crystal approximation. This simple approximation of an alloy of two elements (that differ in nuclear charge with one) is suitable, since the averaging of the nuclear charge and the valence electrons in the model neglects other effects than the band filling.

In the 4d transition series the (hypothetical) $Mo_{0.25}Tc_{0.75}$ alloy has a vanishing ΔE and as Fig. 8 shows, also a low C'. However, the elastic shear constant C' is far from zero, since although ΔE is zero (or almost zero) there is still an energy barrier between the fcc and bcc structures. The main contribution to this energy barrier comes from the Madelung energy, as Fig. 7 shows. Nevertheless, the trend of C' tracks ΔE (roughly), and the dip shown by C' for the $Mo_{0.25}Tc_{0.75}$ alloy is clearly correlated with ΔE being very low.

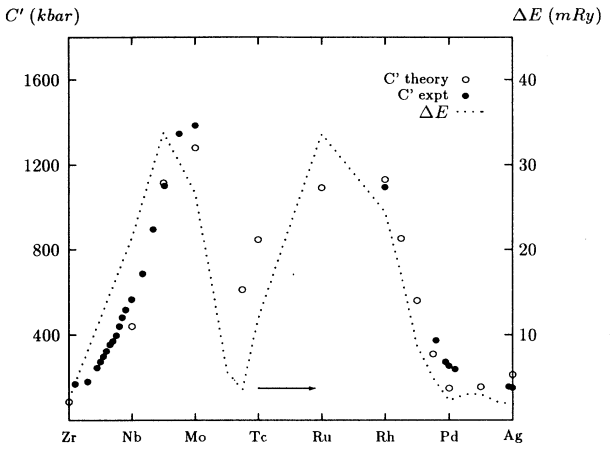

FIG. 8. Experimental (●) and theoretical (○) tetragonal shear constant in kbar and fcc-bcc energy difference (dotted line) in mRy for the 4*d* elements. The bcc energy is lower for Nb and Mo.

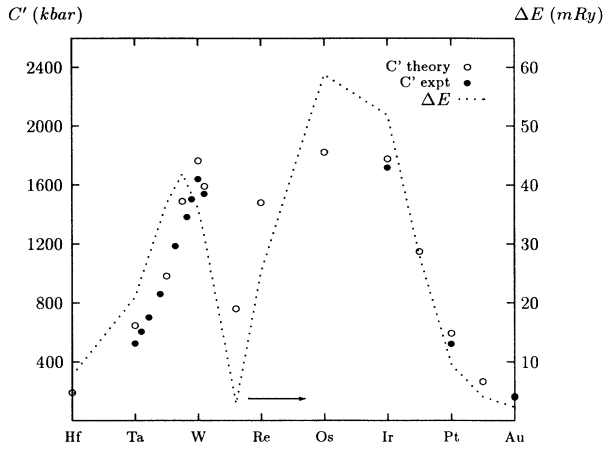

FIG. 9. Experimental (●) and theoretical (○) tetragonal shear constant in kbar and fcc-bcc energy difference (dotted line) in mRy for the 5*d* elements. The bcc energy is lower for Ta and W.

We have also performed calculations for 4*d* alloys where experimental data are available, as well as for (hexagonal) Zr, Tc, and Ru treated as fcc, to study trends. The theoretical and measured elastic shear constant, together with the theoretical ΔE, is thus presented in Fig. 8 for the 4*d* transition elements, complemented with selected alloys. Notice that, when a comparison is possible, the agreement between experiment and theory is good.

Also, it is interesting to notice that in the beginning of the 4*d* transition series the alloy with as much as 90% Zr (hexagonal) and 10% Nb (bcc) is bcc, and the elastic shear constant has been measured.[25] From this alloy C' increases continuously for increasing band filling up to Mo, tracing ΔE. Notice in Fig. 8 that the elastic shear constant thus roughly follows the same trend as ΔE. However, the maximum of the C' curve is at a slightly larger atomic number than the maximum in the ΔE curve, indicating that the shape of the Bains path is not quite the same for all systems. For the Rb_xPd_{1-x} and Pd_xAg_{1-x} alloys the scaling between C' and ΔE also holds and, because of the behavior of ΔE, C' decreases rapidly with increasing band filling.

In Fig. 9 we have plotted the same properties as in Fig. 8, but now for the 5*d* transition series. Here (hexagonal) Hf, Re, and Os were also treated in a hypothetical fcc structure. The elastic shear constant C' for the 5*d* elements displays a similar trend as the 4*d* series does, and the small C' of the $W_{0.36}Re_{0.64}$ alloy corresponds to a low (zero) ΔE (similar to the $Mo_{0.25}Tc_{0.75}$ alloy in the 4*d* series). Notice that the trend of C' is very similar for the 4*d* and 5*d* series, and that C' tracks (roughly) ΔE. However, also for the 5*d* series one can notice that the maximum of the C' curve appears for a slightly higher atomic number than the maximum for ΔE, again indicating that the shape of the total energy along the Bains path is not quite the same for all systems. Nevertheless, we reproduce the experimental finding of a decrease of C' when small amounts of Re is alloyed in W.

IV. CONCLUSIONS

To conclude, we have calculated the elastic constants (C_{11}, C_{12}, and C_{44}) for all nonmagnetic cubic transition elements, and found agreement within $\sim 10\%$ (with a few exceptions). In particular our calculations reproduce the anomalously high C_{11} values found in Rh, Ir, Mo, and W, and we show that is due to an anomalously high C' constant for these systems. Further, we have obtained values of C' in good agreement with experiment, for selected 4*d* and 5*d* transition-metal alloys. We have shown that there is a simple explanation for the trend in C' for the cubic transition metals and alloys. From the calculation of the energy along the Bains path one obtains not only the crystal structure stability, but its "excited" state (ΔE) and the fact that C' is related to its excited state structure. Therefore, unlike V_{eq}, B, and E_c, the crystal structure energies determine the trends in C' and one does not get a parabolic trend. Because both the stable crystal structure and its excited state can be correlated with *d*-band filling we arrive at a simple explanation for the values of C', i.e., *those crystals for which band filling arguments dictate a large ΔE will have large C' values.* The physical explanation for this is that it is precisely these systems for which the bcc→fcc transformation is difficult and hence the C' values high. *The reason for the anomalously high value of C', for Rh, Ir, Mo, W, and alloys that have a dominating concentration of these elements, does thus not depend on whether bonding or antibonding orbitals are being filled* (as in the explanation of V_{eq}, B, and E_c—Friedel model), but rather on details in the DOS, which in turn, depending on band filling, can make the bcc structure very stable against the fcc structure, and vice versa. In connection to this it is very interesting that central force potential calculations do not reproduce the anomalously high C' values found for Ir, Rh, W, and Mo (Fig. 1), and not even the trend, whereas

a theory that takes into account the detailed shape of the DOS (band calculations) explains those irregularities as well as the general trend. We have also predicted an anomalously low elastic shear constant for Mo-Tc (Tc rich) alloys as well as for W-Re (Re rich) alloys, and it would be interesting if these alloys could be stabilized in a cubic structure, and the elastic constants measured.

Finally, there is no (to our knowledge) simple transformation path which, in a similar way to relating the Bains path to the C' constant, connects the C_{44} constant with some crystallographic transformation path. The trend of C_{44} also has less structure than C'. Nevertheless, C_{44} is enhanced compared to the trends expected from B, V_{eq}, and E_c, for Rh, Ir, Mo, and W. The explanation for this enhancement is similar to the arguments for the enhanced values of C'. Namely, taking W as an example, the bcc structure is stable against the fcc structure since, for this band filling, the DOS has most weight at low energies causing E_b to stabilize this structure. However, any type of shear that, for a certain band filling, moves weight of the DOS to higher energies will lower the band energy E_b in Eq. (1). The shear corresponding to C_{44} creates such a change of the DOS for W, and consequently is C_{44} also anomalously high for this particular element.

To summarize, both the shape of the DOS and the particular band filling, i.e., the position of the Fermi level, E_F, is of importance for the elastic shear constant C' as well as the elastic constant C_{44}. For elements such as Mo and Rh in the 4*d* transition series and W and Ir in the 5*d* transition series the *d*-band filling together with the *d*-projected DOS makes the elements exceptionally stable in their true crystal structures and C' as well as C_{44} show exceptionally large values for these metals.

ACKNOWLEDGMENTS

Duane Wallace, Börje Johansson, and R. Schwarz are acknowledged for their critical reading of the manuscript. Valuable discussions with Bengt Nolăng, Bob Albers, Barry Cooper, and Matthew Steiner are acknowledged.

*Present address: Department of Physics, Uppsala University, Uppsala, Sweden.

[1]J. Friedel, *The Physics of Metals,* edited by J. M. Ziman (Cambridge University Press, New York, 1969).

[2]This model was further elaborated on by D. G. Pettifor, in *Solid State Physics,* edited by H. Ehrenreich and D. Turnbull (Academic, New York, 1987), Vol. 40, p. 43.

[3]R. C. Albers, A. M. Boring, and J. C. Boettger, *Advances in Quantum Chemistry* (Academic, New York, 1990), Vol. 21, p. 365.

[4]J. R. Smith, J. Fernante, and J. H. Rose, Phys. Rev. B **25**, 1419 (1982).

[5]J. M. Wills (unpublished).

[6]S. S. Hecker, D. L. Rohr, and F. Stein, Metall. Trans. A **9a**, 481 (1978); D. L. Rohr, L. E. Murr, and S. S. Hecker, *ibid.* **10a**, 399 (1979).

[7]E. S. Machlin and J. Shao, J. Phys. Chem. Solids **44**, 435 (1983).

[8]J. M. Wills, O. Eriksson, P. Söderlind, and A. M. Boring, Phys. Rev. Lett. **68**, 2802 (1992).

[9]M. Dacorogna, J. Ashkenazi, and M. Peter, Phys. Rev. B **26**, 1527 (1982).

[10]N. E. Christensen, Solid State Commun. **49**, 701 (1984); **50**, 177 (1984); Phys. Rev. B **29**, 5547 (1984); Ψ_k-Newslett. **8**, 2 (1984).

[11]Duane C. Wallace, *Thermodynamics of Crystals* (Wiley, New York, 1972).

[12]I. C. Bain, Trans. Metall. Soc. AIME **70**, 25 (1924).

[13]H. L. Shriver, Phys. Rev. B **31**, 1909 (1985).

[14]J. C. Duthie and D. G. Pettifor, Phys. Rev. Lett. **38**, 564 (1977).

[15]G. W. Fernando, R. E. Watson, M. Weinert, Y. J. Wang, and J. W. Davenport, Phys. Rev. B **41**, 11 813 (1990); R. E. Watson, G. W. Fernando, M. Weinert, Y. J. Wang, and J. W. Davenport, *ibid.* **43**, 1455 (1991); A. T. Paxton, M. Methfessel, and H. M. Polatoglou, *ibid.* **41**, 8127 (1990).

[16]O. K. Andersen, Phys. Rev. B **12**, 3060 (1975).

[17]H. L. Skriver, *The LMTO Method* (Springer, Berlin, 1984).

[18]M. Shimizu, Physica B **159**, 26 (1989).

[19]Y. Ohta and M. Shimizu, J. Phys. F **13**, 761 (1983).

[20]M. Alouani, R. C. Albers, and M. Methfessel, Phys. Rev. B **43**, 6500 (1991).

[21]J. M. Wills (unpublished); J. M. Wills and B. R. Cooper, Phys. Rev. B **36**, 3809 (1987); D. L. Price and B. R. Cooper, *ibid.* **39**, 4945 (1989).

[22]D. J. Chadi and M. L. Cohen, Phys. Rev. B **8**, 5747 (1973); S. Froyen, *ibid.* **39**, 3168 (1989).

[23]V. L. Moruzzi, J. F. Janak, and A. R. Williams, *Calculated Electronic Properties of Metals* (Pergamon, New York, 1978).

[24]E. Esposito, A. E. Carlson, D. D. Ling, H. Ehrenreich, and C. D. Gelat, Philos. Mag. A **41**, 251 (1980).

[25]R. F. S. Hearmon, *Landolt-Börnstein, Numerical Data and Functional Relationships in Science and Technology, Vol. 11: Magnetic Properties of Coordination and Organometallic Transition Metal Compounds,* edited by K.-H. Hellwege and A. M. Hellwege (Springer, Berlin, 1979).